

# Synthesis of $^{11}\text{C}$ -labelled (*R*)-OHDMI and CFMME and their evaluation as candidate radioligands for imaging central norepinephrine transporters with PET

Magnus Schou,<sup>a,b,\*</sup> Victor W. Pike,<sup>b</sup> Judit Sóvágó,<sup>a</sup> Balázs Gulyás,<sup>a</sup> Peter T. Gallagher,<sup>c</sup> David R. Dobson,<sup>c</sup> Magnus W. Walter,<sup>c</sup> Helene Rudyk,<sup>c</sup> Lars Farde<sup>a</sup> and Christer Halldin<sup>a</sup>

<sup>a</sup>Karolinska Institutet, Department of Clinical Neuroscience, Psychiatry Section, Karolinska Hospital, S-17176 Stockholm, Sweden

<sup>b</sup>Molecular Imaging Branch, National Institute of Mental Health, National Institutes of Health, Bethesda, MD 20892-1003, USA

<sup>c</sup>Eli Lilly Co, Erl Wood Manor, Windlesham, Surrey GU20 6PH, UK

Received 2 June 2006; revised 23 October 2006; accepted 31 October 2006

Available online 2 November 2006

**Abstract**—(*R*)-1-(10,11-Dihydro-dibenzo[*b,f*]azepin-5-yl)-3-methylamino-propan-2-ol ((*R*)-OHDMI) and (*S,S*)-1-cyclopentyl-2-(5-fluoro-2-methoxy-phenyl)-1-morpholin-2-yl-ethanol (CFMME) were synthesized and found to be potent inhibitors of norepinephrine reuptake. Each was labelled efficiently in its methyl group with carbon-11 ( $t_{1/2} = 20.4$  min) as a prospective radioligand for imaging brain norepinephrine transporters (NET) with positron emission tomography (PET). The uptake and distribution of radioactivity in brain following intravenous injection of each radioligand into cynomolgus monkey was examined *in vivo* with PET. After injection of (*R*)-[ $^{11}\text{C}$ ]OHDMI, the maximal whole brain uptake of radioactivity was very low (1.1% of injected dose; I.D.). For occipital cortex, thalamus, lower brainstem, mesencephalon and cerebellum, radioactivity ratios to striatum at 93 min after radioligand injection were 1.35, 1.35, 1.2, 1.2 and 1.0, respectively. After injection of [ $^{11}\text{C}$ ]CFMME, radioactivity readily entered brain (3.5% I.D.). Ratios of radioactivity to cerebellum at 93 min for thalamus, occipital cortex, region of locus coeruleus, mesencephalon and striatum were 1.35, 1.3, 1.3, 1.2 and 1.2, respectively. Radioactive metabolites in plasma were measured by radio-HPLC. (*R*)-[ $^{11}\text{C}$ ]OHDMI represented 75% of plasma radioactivity at 4 min after injection and 6% at 30 min. After injection of [ $^{11}\text{C}$ ]CFMME, 84% of the radioactivity in plasma represented parent at 4 min and 20% at 30 min. Since the two new hydroxylated radioligands provide only modest regional differentiation in brain uptake and form potentially troublesome lipophilic radioactive metabolites, they are concluded to be inferior to existing radioligands, such as (*S,S*)-[ $^{11}\text{C}$ ]MeNER, (*S,S*)-[ $^{18}\text{F}$ ]FMeNER-D<sub>2</sub> and (*S,S*)-[ $^{18}\text{F}$ ]FRB-D<sub>4</sub>, for the study of brain NETs with PET *in vivo*.

© 2006 Elsevier Ltd. All rights reserved.

## 1. Introduction

Norepinephrine transporters (NETs) are pre-synaptic membrane glycoproteins that are mainly localized within a small brainstem region, the locus coeruleus.<sup>1,2</sup> NETs have been implicated in the pathophysiology of several neuropsychiatric and neurodegenerative disorders.<sup>3–6</sup> Furthermore, over the past decades NET inhibitors have been used in treating depression and lately have been suggested for treating attention deficit hyperactivity disorder (ADHD).<sup>7</sup> Hence, there is considerable inter-

est to image brain NET with positron emission tomography (PET) or single photon emission tomography (SPET) in clinical research, especially on depression and ADHD, and in drug development.

Attempts to image NET in the human brain *in vivo* with PET have so far met with limited success, despite recently increased efforts. Four years ago, only one candidate radioligand, [ $^{11}\text{C}$ ]nisoxetine ([ $^{11}\text{C}$ ]NXT), had been evaluated *ex vivo*<sup>8</sup> but since then about thirteen others have been evaluated, including [ $^{11}\text{C}$ ]desipramine ([ $^{11}\text{C}$ ]DMI),<sup>9</sup> [ $^{125}\text{I}$ ]INXT (*ex vivo*),<sup>10,11</sup> (*R*)-[ $^{11}\text{C}$ ]NXT,<sup>12</sup> [ $^{11}\text{C}$ ]lortalamine,<sup>12</sup> [ $^{11}\text{C}$ ]oxaprotiline,<sup>12</sup> [ $^{11}\text{C}$ ]talopram,<sup>9,13</sup> [ $^{11}\text{C}$ ]tal-supram,<sup>9,13</sup> two  $^{11}\text{C}$ -labelled analogues of mazindol<sup>14</sup> and some  $^{11}\text{C}$ -labelled<sup>12,15–17</sup> and  $^{18}\text{F}$ -labelled<sup>12,18</sup> analogues of the antidepressant, reboxetine (Edronax<sup>®</sup>).

**Keywords:** NET; Radioligand; PET; Brain.

\* Corresponding author. Tel.: +46 8 51772675; fax: +46 8 51771753; e-mail: [magnus.schou@ki.se](mailto:magnus.schou@ki.se)

Of these radioligands, the reboxetine analogues, (*S,S*)-[<sup>11</sup>C]MeNER,<sup>15–17</sup> (*S,S*)-[<sup>18</sup>F]FMeNER-D<sub>2</sub><sup>18,19</sup> and (*S,S*)-[<sup>18</sup>F]FRB-D<sub>4</sub><sup>12</sup> are able to image NET in vivo but not with high sensitivity.

We considered DMI (**1**, Fig. 1) and (*S,S*)-MeNER (**3**, Fig. 1) still to be useful lead compounds for the development of improved PET radioligands, given their high affinities (IC<sub>50</sub>s of 0.97 and 2.5 nM, respectively) and selectivities for NET, and in particular (*S,S*)-MeNER, in view of its appreciable efficacy when labelled with carbon-11 (*t*<sub>1/2</sub> = 20.4 min) as a PET radioligand.

Although not clearly verified experimentally, it is generally considered that the non-specific binding of a radioligand in brain in vivo will increase with the lipophilicity of the radioligand. DMI is a rather lipophilic compound as indexed by its calculated octanol–water partition coefficient (clog *P* = 4.00). In comparison, MeNER appears to have appreciably lower lipophilicity (clog *P* = 2.55). We wished to test whether a reduction in lipophilicity with retention of NET binding affinity in a <sup>11</sup>C-labelled analogue of DMI might increase the ratio of specific to non-specific binding in PET experiments (by reducing non-specific binding). For this purpose, we considered that the introduction of a hydroxyl group into candidate radioligands might serve as a strategy to reduce lipophilicity.

DMI is a NET inhibitor with a fused tricyclic core that somewhat resembles that in hydroxy-maprotiline (OXA, **2**, Fig. 1). Whereas DMI is achiral, OXA is chiral and its binding to NET is highly stereoselective with the (*S*)-enantiomer being the more potent (IC<sub>50</sub> = 1.1 nM; eudismic ratio ~1000).<sup>20,21</sup> Hydroxylation of the ring structure of DMI is known to reduce affinity towards NET by about 3-fold.<sup>22</sup> High affinity is of paramount importance in prospective radioligands for imaging low concentrations of target protein, such as NET. Hence, ring hydroxylation was ruled out of consideration for new radioligand development. Nevertheless, given the overall structural similarity of DMI to OXA, we predicted that hydroxylation of DMI at the β-position of the *N*-methyl aminopropyl group might well be tolerated for binding to NET. The chemistry for producing β-hydroxylated DMI derivatives has been described earlier.<sup>23,24</sup> However, the potencies of such compounds for NET inhibition had not been reported. We expected that the binding of a β-hydroxylated DMI (**4**, Fig. 1) to NET would be of high affinity and also stereoselective by analogy with the properties of OXA.

MeNER is a NET inhibitor without a fused tricyclic core.<sup>25</sup> The binding of MeNER to NET is stereoselective both in vitro and in vivo; the *S,S*-enantiomer (**3**, Fig. 1) is the more potent with a eudismic ratio of about 20 in vitro.<sup>26</sup> Investigations of structure–activity relationships on the aryloxy morpholine scaffold (Eli Lilly Co.; unpublished results) have shown that some elaborate alterations to MeNER, extra to hydroxylation, are tolerated for high affinity binding to NET. (*S,S*)-Cyclopentyl-2-(5-fluoro-2-methoxy-phenyl)-1-morpholin-2-yl-etha-

nol (CFMME, **5**, Fig. 1) is a potent (IC<sub>50</sub> = 10.8 nM) and selective NET inhibitor, which may be considered to be derived from MeNER through hydroxylation and other structural modifications. The clog *P* (2.37) of CFMME is similar to that of MeNER. We were interested to see if the presence of an hydroxy group in this compound would have a beneficial effect on the ratio of NET-specific to non-specific binding in vivo.

We aimed to prepare and evaluate two novel <sup>11</sup>C-labelled NET ligands, one analogue of DMI, namely [<sup>11</sup>C](*R*)-1-(10,11-dihydro-dibenzo[*b,f*]azepin-5-yl)-3-methylamino-propan-2-ol ((*R*)-[<sup>11</sup>C]OHDMI; [*N*-methyl-<sup>11</sup>C]**4**), and one tertiary alcohol, namely [<sup>11</sup>C]CFMME ([*O*-methyl-<sup>11</sup>C] **5**), as candidate radioligands for PET imaging of NET.

## 2. Results

### 2.1. Chemistry

(*R*)-OHDMI (**4**) and its nor-methyl precursor (**8**) were synthesized from iminodibenzyl in two and three steps in 10 and 15% overall yield, respectively, by adapting the methods of Levy et al.<sup>23</sup> and Schindler and Hafliger (Scheme 1).<sup>24</sup> The key intermediate, homochiral epoxide **6**, was obtained by treating iminodibenzyl with (*S*)-epichlorohydrin.<sup>23</sup> (*S*)-OHDMI was prepared similarly from (*R*)-epichlorohydrin. It may be noted that although configuration is retained in the reaction between iminodibenzyl and chiral epichlorohydrin, the required prioritization of the substituents on the chiral centre dictates that the descriptor for absolute configuration be changed.

### 2.2. Radiochemistry

(*R*)-[<sup>11</sup>C]OHDMI was obtained in a quantitative radiochemical yield from [<sup>11</sup>C]methyl triflate. The radioligand was obtained within 30 min after the end of radionuclide production with a radiochemical purity exceeding 99% (*t*<sub>R</sub> = 4.2 min). The specific radioactivity of (*R*)-[<sup>11</sup>C]OHDMI was 390 GBq/μmol (10.0 Ci/μmol) at the time of administration and less than 2.5 μg/mL of non-labelled precursor (**8**) was present in the product formulation.

[<sup>11</sup>C]CFMME was obtained quantitatively from [<sup>11</sup>C]methyl iodide within 30 min from the end of radionuclide production with a radiochemical purity exceeding 99% (*t*<sub>R</sub> = 3.4 min). The specific radioactivity of [<sup>11</sup>C]CFMME at time of injection was 170 GBq/μmol (4.7 Ci/μmol) and less than 1 μg/mL of non-labelled precursor (**10**) was present in the product formulation.

Both radioligands were stable in the sterile physiological buffer solution for the duration of the experiment (radiochemical purity > 99% at 90 min).

### 2.3. clog *P* calculations and log *D*<sub>7,4</sub> measurements

The clog *P* values of OHDMI and CFMME were calculated to be 2.97 and 2.37 and the clog *D*<sub>7,4</sub> values 0.66

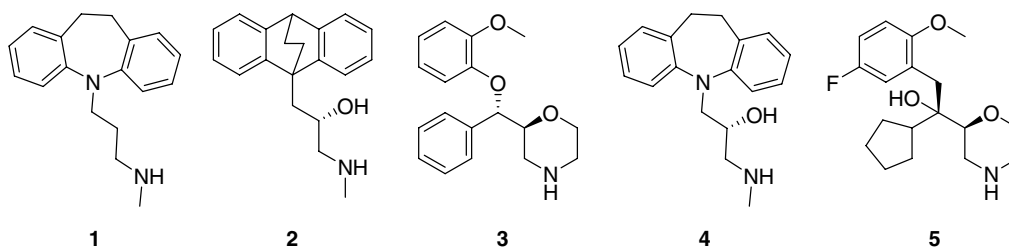
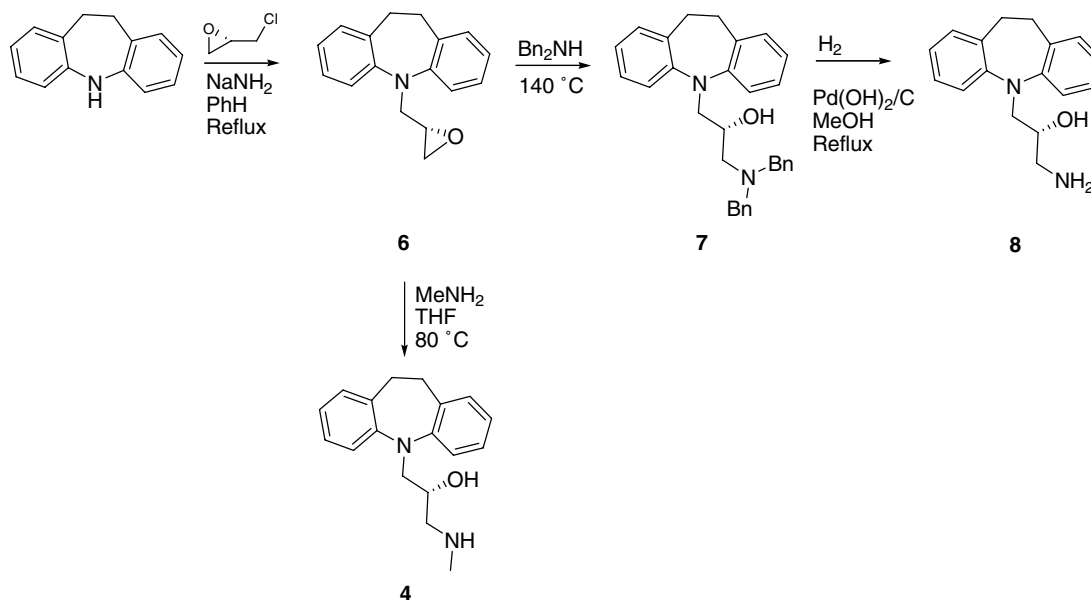


**Figure 1.** Structures of NET inhibitors: DMI (1), OXA (2), (S,S)-MeNER (3), (R)-OHDMI (4), CFMME (5).



**Scheme 1.** Synthesis of (R)-OHDMI (4) and its nor-precursor (8).

and 1.05, respectively. The corresponding empirically obtained values for  $\log D_{7.4}$  of OHDMI and CFMME were 1.28 and 1.63, respectively.

#### 2.4. Pharmacology

(R)-OHDMI and CFMME had no detectable affinity towards dopamine transporters and were found to be 5.5- and 40.3-fold selective towards the serotonin transporters, respectively. The  $K_{is}$  of (R)-OHDMI and CFMME at NET were 8.29 and 10.8 nM, respectively. The inhibitory constants of DMI and (S,S)-MeNER in the same assay were 1.00 and 7.93 nM, respectively.

#### 2.5. PET measurements

Following intravenous injection of (R)-[<sup>11</sup>C]OHDMI (52 MBq; 0.05 μg carrier), radioactivity entered brain to a very limited extent, with a peak of 1.1% of the injected dose present in brain at 80 min after injection. The rank order for radioactivity accumulation in different brain regions was: occipital cortex > thalamus ~ mesencephalon ~ lower brainstem > striatum ~ cerebellum (Figs. 2 and 3). Radioactivity ratios to striatum at the end of the PET measurement (93 min) were 1.35, 1.35, 1.2, 1.2 and 1.0 for occipital cortex, thalamus, lower brainstem, mesencephalon and cerebellum, respectively.

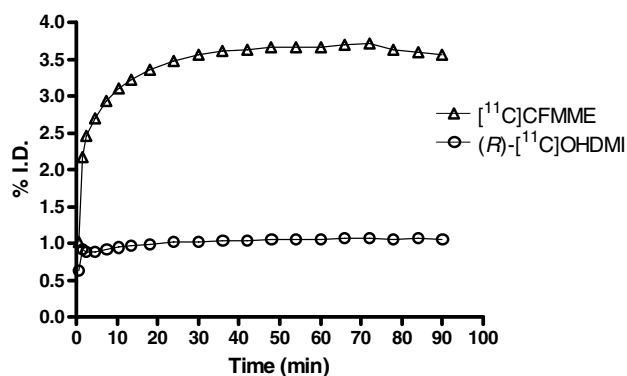


**Figure 2.** Whole brain uptake of radioactivity as percent of injected dose (%I.D.) following injection of (R)-[<sup>11</sup>C]OHDMI and [<sup>11</sup>C]CFMME.

Following intravenous injection of [<sup>11</sup>C]CFMME (50 MBq; 0.1 μg carrier), radioactivity readily entered brain with a peak uptake of about 3.5% of the injected dose at 24 min after injection. The rank order of radioactivity uptake in the different brain regions was: thalamus > occipital cortex ≈ region of locus coeruleus > mesencephalon ≈ striatum > cerebellum (Figs. 2 and 3). Radioactivity ratios to cerebellum were 1.35, 1.3, 1.3, 1.2 and 1.2 at 93 min for thalamus, occipital cortex,

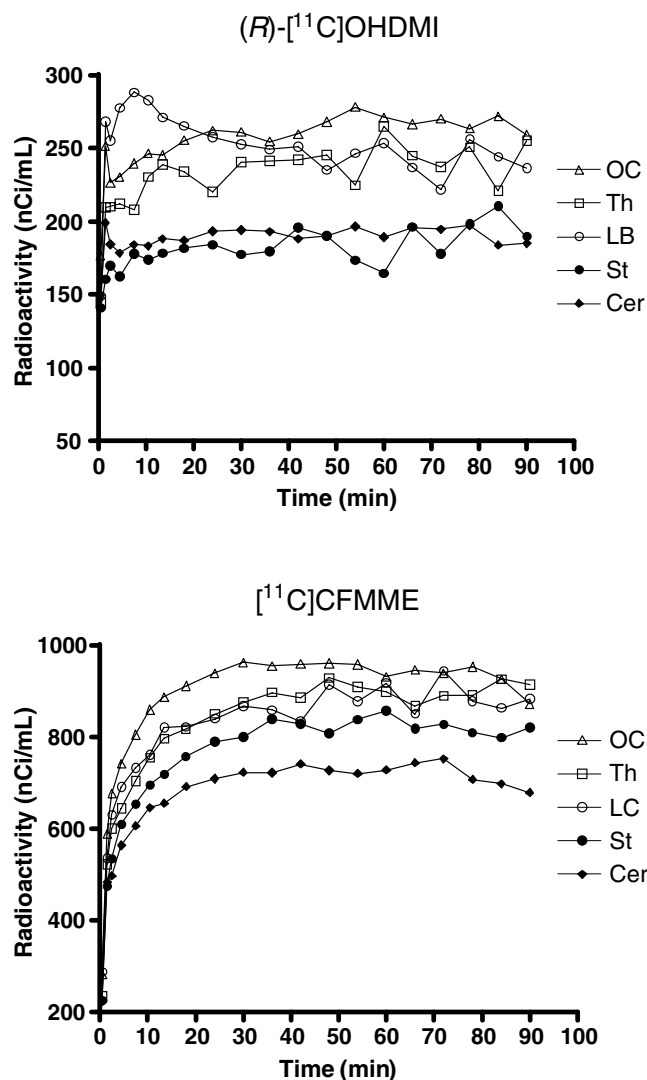


**Figure 3.** Regional brain distribution following injection of (*R*)-[<sup>11</sup>C]OHDMI and [<sup>11</sup>C]CFMME. Abbreviations: Cer, cerebellum; LC, region contain the locus coeruleus; OC, occipital cortex; St, striatum; Th, thalamus.

region of locus coeruleus, mesencephalon and striatum, respectively.

### 2.6. Analysis of radiometabolites in plasma and determination of free fraction

After injection of (*R*)-[<sup>11</sup>C]OHDMI into monkey, unchanged radioligand ( $t_R = 5.7$  min) represented 75% of the radioactivity in plasma at 4 min and 6% at 30 min. Two other radioactive fractions eluted from the HPLC column. One fraction eluted unretained and represented 16% of the plasma radioactivity at 4 min and 93% at 30 min. The other fraction ( $t_R = 5$  min) decreased from 9% of the radioactivity in plasma at 4 min to 1% at 30 min.

After injection of [<sup>11</sup>C]CFMME, the radioactivity in plasma corresponding to unchanged radioligand ( $t_R = 6.0$  min) was 84% at 4 min, 48% at 15 min and

20% at 30 min. At 4 min after injection of [<sup>11</sup>C]CFMME, a significant portion, (10%) of the radioactivity in plasma, was more lipophilic ( $t_R = 7.5$  min) than parent radioligand. A more polar radiometabolite, which eluted unretained from the HPLC column, increased from 6% of the total radioactivity at 4 min to 52% at 15 min and 80% at 30 min.

The free fraction of (*R*)-[<sup>11</sup>C]OHDMI and [<sup>11</sup>C]CFMME in monkey plasma was 51% and 32%, respectively.

## 3. Discussion

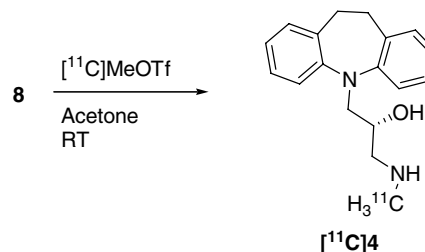
### 3.1. Chemistry

The enantiomers of OHDMI and of the corresponding desmethyl precursors were successfully obtained according to Scheme 1. Reactions of epichlorohydrin with secondary amines are known to proceed through an intermediate  $\alpha$ -chloro alcohol that cyclizes with retention of absolute configuration to afford chiral epoxides in high enantiomeric excess.<sup>27,28</sup> Accordingly, retention of configuration was also observed by Levy et al. in the epoxide product (**6**) from the reaction between iminodibenzyl and epichlorohydrin.<sup>23</sup> Ring opening of the resultant chiral epoxide by, for example, nucleophilic attack of an amine is regioselective for the least hindered secondary carbon of the epoxide and results in retention of absolute configuration in the generated alcohol.<sup>24,28</sup> Thus, to avoid the need to achieve a chiral separation of the (*R*)-enantiomer of the amine precursor (**8**) or of [<sup>11</sup>C]OHDMI itself, we decided to obtain **8** from the easily prepared homochiral epoxide, **6**. The latter was also readily converted into the reference ligand, **4**. Antipodes of the precursor **8** and ligand **4** were likewise obtained, starting from iminodibenzyl and (*R*)-epichlorohydrin.

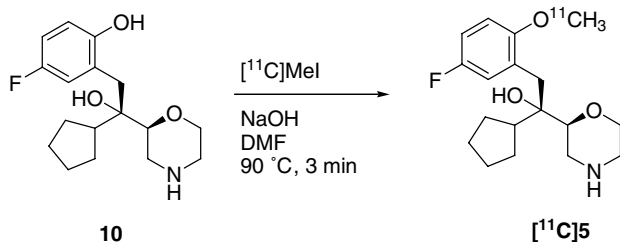
### 3.2. Radiochemistry

(*R*)-[<sup>11</sup>C]OHDMI was prepared by rapid alkylation of the nor-precursor **8** with [<sup>11</sup>C]methyl triflate under mild conditions (Scheme 2). A quantitative decay-corrected radiochemical yield was achieved without addition of another base.

[<sup>11</sup>C]CFMME was rapidly and efficiently prepared from the unprotected precursor phenol **10**, under conditions similar to those previously used to produce (*S,S*)-[<sup>11</sup>C]MeNER (Scheme 3).<sup>15</sup> As in the preparation of



**Scheme 2.** Labelling of (*R*)-[<sup>11</sup>C]OHDMI ([<sup>11</sup>C]**4**).



Scheme 3. Labelling of [ $^{11}\text{C}$ ]CFMME ([ $^{11}\text{C}$ ]5).

(*S,S*)-[ $^{11}\text{C}$ ]MeNER, accompanying *N*-methylation of the morpholino nitrogen was not observed.

### 3.3. *clog P* calculations and $\log D_{7.4}$ measurements

The *clog P* and *clog D*<sub>7.4</sub> calculations predicted OHDMI to be less lipophilic than DMI, and CFMME less lipophilic than MeNER. In line with these calculated values, empirically determined  $\log D_{7.4}$  also showed decreased lipophilicity for CFMME and OHDMI. However, there was also a discrepancy of about 0.6 U between the predicted values of  $\log D_{7.4}$  and the measured values. Computer-generated estimates of  $\log P$  as indexes of lipophilicity are useful guides in radioligand development, especially ahead of ligand synthesis, but clearly they may not be relied on alone.

### 3.4. Pharmacology

CFMME ( $K_i = 10.8$  nM) and (*R*)-OHDMI ( $K_i = 8.29$  nM) were found to be only very slightly less potent than (*S,S*)-MeNER ( $K_i = 7.93$  nM) in the same assay. However (*R*)-OHDMI ( $K_i = 8.29$  nM) was found to be about eight times less potent than DMI ( $K_i = 1.00$  nM). Thus, counter to our hypothesis, hydroxylation of the  $\beta$ -position of the aminopropyl side chain of DMI appears to be less tolerated with regard to binding to NET than hydroxylation of the aromatic moiety.

A remarkable observation is that, whereas MeNER was found to be about three times more potent than DMI in the original paper by Melloni et al.<sup>25</sup> it was found to be equipotent to (*R*)-OHDMI in the assay used for this study and thus about eight times less potent than DMI. The reason for this apparent discrepancy remains unclear. In general, *in vitro* affinity data may vary greatly in the literature and thus require cautious interpretation.

### 3.5. PET measurements

After intravenous injection of (*R*)-[ $^{11}\text{C}$ ]OHDMI into cynomolgus monkey, the accumulation of radioactivity in brain was slow and reached only 1.1% of the injected radioactivity at 80 min (Fig. 2). By contrast, after injection of cynomolgus monkey with [ $^{11}\text{C}$ ]DMI, about 2.7% of radioactivity entered brain after 24 min.<sup>9</sup> Hence, hydroxylation of [ $^{11}\text{C}$ ]DMI did not improve penetration into monkey brain. The brain uptake of a radioligand

depends on many factors, such as ligand lipophilicity, the plasma free fraction, rate of clearance from blood and substrate affinity for active efflux pumps.<sup>29–31</sup> Of these factors, lipophilicity and plasma free fraction were on a level that should ensure passage through the BBB, whereas the rate of metabolism was very fast. The latter, possibly in combination with active transport out of the brain by an efflux pump, may account for the low brain uptake. The slow accumulation of radioactivity in brain after administration of (*R*)-[ $^{11}\text{C}$ ]OHDMI may well suggest that a significant proportion of the entering radioactivity is associated with radioactive metabolites (*vide infra*).

Although having considerably lower affinity towards NET according to the present assay, greater regional differentiation in brain radioactivity uptake was seen with (*R*)-[ $^{11}\text{C}$ ]OHDMI than previously with [ $^{11}\text{C}$ ]DMI.<sup>9</sup> For example, the ratio of radioactivity in NET-rich thalamus to NET-poor striatum is about 1.35 with (*R*)-[ $^{11}\text{C}$ ]OHDMI compared to 1.15 with [ $^{11}\text{C}$ ]DMI. Although (*R*)-[ $^{11}\text{C}$ ]OHDMI accumulates in NET-rich regions, it does so with less regional differentiation than (*S,S*)-[ $^{11}\text{C}$ ]MeNER, which shows a thalamus to striatum ratio of about 1.5. The low ratios of radioactivity in NET-rich regions to that in striatum or cerebellum result in images with poor contrast (e.g., Fig. 4, panel A). For (*R*)-[ $^{11}\text{C}$ ]OHDMI, it is notable that the level of radioactivity in striatum is similar to that in cerebellum across the full time course of the experiment (Fig. 3, panel A). Striatum and cerebellum have been shown to contain negligible levels of NETs in the primate brain *in vitro*<sup>32</sup> and are therefore considered to be candidate regions to represent non-specific binding for NET radioligands. It is thus remarkable that the high uptake in cerebellum after injection of (*S,S*)-[ $^{11}\text{C}$ ]MeNER in baboons was NET-specific.<sup>17</sup> A possible explanation for this discrepancy is that a difference in regional NET expression exists between monkeys and baboons.

After injection of [ $^{11}\text{C}$ ]CFMME into cynomolgus monkey, radioactivity readily entered brain, with 3.5% of the injected dose present in brain from 42 min until the end of the experiment (Fig. 2). The radioactivity level in brain did not thereafter subside during the PET measurement, which may indicate accumulation of a radiometabolite in brain. The magnitude of brain uptake of radioactivity was similar to that achieved with (*S,S*)-[ $^{11}\text{C}$ ]MeNER (3% of injected dose at 18 min) and is sufficient for a PET radioligand.<sup>15</sup> Radioactivity accumulated in NET-rich brain regions, such as in the region of locus coeruleus<sup>†</sup> and thalamus. However, ratios of radioactivity in NET-rich regions to that in cerebellum were low and maximally 1.35 for thalamus. There was also a significantly higher (ca. 20%) uptake in NET-poor striatum than in cerebellum (Fig. 3, panel B). Several

<sup>†</sup> Since locus coeruleus is such a small region in the monkey brain, the surrounding region was drawn as a region of interest for the determination of radioactivity accumulation in the region.

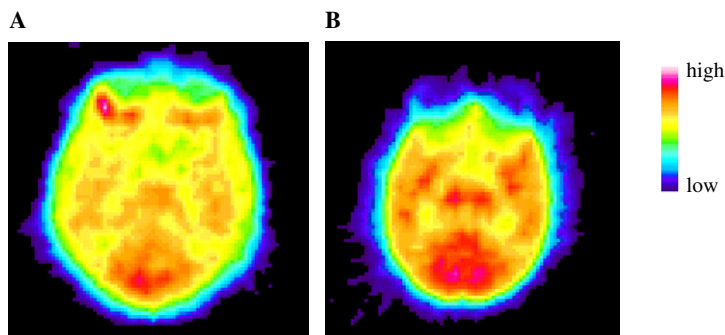


**Figure 4.** Colour-coded horizontal PET images from summed 9–93 min emission data following injection of (*R*)-[<sup>11</sup>C]OHDMI (A) and [<sup>11</sup>C]CFMME (B) at the level of thalamus and striatum.

other candidate radioligands for imaging NET have also shown a higher uptake in striatum than in cerebellum. These include (*R*)-[<sup>11</sup>C]nisoxetine, (*R*)-[<sup>11</sup>C]lortalamine and [<sup>11</sup>C]oxaprotiline,<sup>12</sup> whose uptake in striatum was found to be insensitive to pretreatment with nisoxetine. It is uncertain whether the unexpectedly high accumulation of radioactivity in striatum following administration of [<sup>11</sup>C]CFMME is wholly non-specific binding or whether it also contains specific binding to an unknown high affinity site.

Even if [<sup>11</sup>C]CFMME were to give high NET-specific PET signals in brain *in vivo*, the accumulation of radioactivity in striatum would compromise the utility of this radioligand, since striatum would not represent the non-specific binding in other regions and may not be used as a reference region for deriving parameters related to NET density. PET images obtained with this radioligand show acceptable uptake of radioactivity in brain but low contrast in radioactivity distribution between regions (Fig. 4, panel B). This radioligand is also inferior to the pre-existing radioligands, (*S,S*)-[<sup>11</sup>C]MeNER, (*S,S*)-[<sup>18</sup>F]FRB-D<sub>4</sub> and (*S,S*)-[<sup>18</sup>F]MeNER-D<sub>2</sub>,<sup>15,18</sup> with respect to the magnitudes of the obtainable NET-specific PET signals.

### 3.6. Analysis of radioactive metabolites in plasma and determination of free fraction

Studies of radioactive metabolites are of high importance for PET radioligand development since PET only measures radioactivity and gives no information on the chemical species associated with the radioactivity. Radioligands intended to image a target in brain, such as NET, are unlikely to be successful if they give rise to radioactive metabolites that may enter brain to confound the signal measured with PET. (*R*)-[<sup>11</sup>C]OHDMI was rapidly metabolised, such that it represented only 75% of the radioactivity in plasma at 4 min after injection and only 6% at 30 min. At 4 min after injection of (*R*)-[<sup>11</sup>C]OHDMI, 6% of the radioactivity in plasma corresponded to a radioactive metabolite with lipophilicity similar to that of the parent radioligand, based on its retention time on reverse phase HPLC. It is possible that this radioactive metabolite enters brain to confound PET imaging with (*R*)-[<sup>11</sup>C]OHDMI. Other radioactive metabolites appeared to be much less lipophilic.

In plasma sampled at 4 min after injection of [<sup>11</sup>C]CFMME, 10% of the radioactivity was found to be more lipophilic than the parent radioligand. This fraction was later cleared from plasma and by 30 min the radioactivity in plasma is mainly represented by much less lipophilic metabolites. A similar observation was made in PET measurements with (*S,S*)-[<sup>11</sup>C]MeNER in monkeys and humans. A possible explanation is that the radioactive fraction is a product of Phase I metabolism that subsequently undergoes conjugation to be rendered more hydrophilic. Again it is possible that the early lipophilic radioactive metabolite enters brain to confound PET imaging with [<sup>11</sup>C]CFMME, especially in view of the whole brain uptake curve not showing any wash-out of radioactivity throughout the experiment.

The free fraction of (*R*)-[<sup>11</sup>C]OHDMI and [<sup>11</sup>C]CFMME was high for both radioligands. High plasma protein binding can thus be ruled out as a reason for the low brain uptake of (*R*)-[<sup>11</sup>C]OHDMI.

## 4. Conclusions

One hydroxylated derivative of DMI and one tertiary alcohol derived from the (*S,S*)-MeNER platform were prepared and labelled with carbon-11. The radioligands were evaluated by PET in cynomolgus monkeys and although showing slight regional differentiation in brain uptake of radioactivity, they both suffer from extensive metabolism that includes the formation of lipophilic radioactive metabolites. In addition, (*R*)-[<sup>11</sup>C]OHDMI shows too low accumulation in brain to be useful as a PET radioligand and [<sup>11</sup>C]CFMME shows unexpectedly high binding in striatum. Thus, each is concluded to be inferior to (*S,S*)-[<sup>11</sup>C]MeNER, (*S,S*)-[<sup>18</sup>F]FRB-D<sub>4</sub> or (*S,S*)-[<sup>18</sup>F]MeNER-D<sub>2</sub> as radioligands for imaging NET *in vivo* with PET.

## 5. Materials and methods

### 5.1. Chemistry

**5.1.1. Materials and general procedures.** CFMME hydrochloride (**5**, LY 2152041) and its desmethyl analogue (**10**) were prepared at Eli Lilly Co.<sup>33</sup> All reagents and solvents, including anhydrous solvents, were obtained from Sig-

ma–Aldrich (Sweden) and used without further purification. Reactions were performed under a dry inert atmosphere with dry solvent, unless otherwise stated. TLC was performed on silica gel (60 F254; Merck) with detection under UV light or by charring with ethanolic phosphomolybdic acid. Flash column chromatography was performed on silica gel (60 Å; 70–230 mesh; Sigma–Aldrich).  $^1\text{H}$  NMR spectra (400 MHz) were recorded on a drx400 spectrometer (Bruker, Germany) as solutions of test compound in  $\text{CDCl}_3$  [residual  $\text{CHCl}_3$  ( $\delta$  7.27) as internal standard] or  $\text{DMSO-}d_6$  [residual  $\text{DMSO-}d_5$  ( $\delta$  2.50) as internal standard] at 300 K.  $^{13}\text{C}$  NMR spectra (100 MHz) were recorded on the same spectrometer as solutions of test compounds in  $\text{CDCl}_3$  [residual  $\text{CHCl}_3$  ( $\delta$  77.34) as internal standard] or  $\text{DMSO-}d_6$  [residual  $\text{DMSO-}d_5$  ( $\delta$  40.76) as internal standard] at 300 K. Mass spectra were acquired on a quadrupole-orthogonal injection time-of-flight (TOF) mass spectrometer (QTOF1; Waters-Micro-mass Plc, Manchester, UK). Samples were sprayed from gold-plated borosilicate capillaries (Protana AS, Odense, Denmark) using a capillary voltage of +1 kV.

**5.1.1.1. (R)-5-Oxiranylmethyl-10,11-dihydro-5H-dibenzo[b,f]azepine (6).**<sup>23</sup> A suspension of sodamide (300 mg; 7.7 mmol) in toluene was added dropwise to a solution of iminodibenzyl (1 g; 5.12 mmol) and (*S*)-epichlorohydrin (474 mg; 5.12 mmol) in benzene (50 mL). The mixture was refluxed for 6 h and then solvents, removed under reduced pressure. The residue was washed with hydrochloric acid (0.1 M) and extracted with dichloromethane. The organic layer was dried ( $\text{Na}_2\text{SO}_4$ ). The crude product was purified by flash chromatography on silica gel (hexanes  $\rightarrow$  hexanes–EtOAc 20:1 v/v) to yield **6** as a white powder (580 mg; 45%).  $^1\text{H}$  NMR: 7.07 (m, 6H), 6.92 (m, 2H), 3.90 (m, 2H), 3.17 (s, 4H), 3.05 (m, 1H), 2.69 (t,  $J = 4.3$  Hz, 1H), 2.55 (m, 1H).

**5.1.1.2. (R)-1-(10,11-Dihydro-dibenz[b,f]azepin-5-yl)-3-dibenzylamino-propan-2-ol (7).** The epoxide **6** (580 mg; 2.31 mmol) and dibenzylamine (1.370 g; 6.93 mmol) were mixed and heated at 140 °C overnight. The crude product was purified by flash chromatography on silica gel (hexanes  $\rightarrow$  hexanes–EtOAc, 6:1 v/v) to yield **7** as a pale oil that crystallized upon standing in the freezer (480 mg; 46%).  $^1\text{H}$  NMR: 7.2–7.4 (m, 10H), 7.1 (m, 6H), 6.9 (m, 2H), 3.9 (m, 1H), 3.8 (m, 2H), 3.6 (d,  $J = 10.8$  Hz, 2H), 3.4 (d,  $J = 10.8$  Hz, 2H), 3.1 (s, 4H), 2.6 (dd,  $J = 4.6, 11.6$  Hz, 1H), 2.4 (m, 1H).  $^{13}\text{C}$  NMR: 148.6, 138.8, 134.6, 130.3, 129.5, 128.9, 128.9, 127.7, 126.9, 123.3, 120.3, 65.3, 59.1, 58.3, 55.7, 35.6. MS (TOF) 448.2517 (anal.) 448.2515 (calcd).

**5.1.1.3. (R)-1-(10,11-Dihydro-dibenz[b,f]azepin-5-yl)-3-methylamino-propan-2-ol (4).** A stirred solution of epoxide **6** (580 mg; 2.31 mmol) and methylamine (7 mL; 2 M in THF) was heated at 90 °C in a sealed vessel for 4 h and then solvent evaporated off. The crude product was purified by flash chromatography on silica gel ( $\text{CH}_2\text{Cl}_2 \rightarrow \text{CH}_2\text{Cl}_2\text{-MeOH-c. NH}_4\text{OH}$ , 9:1:0.1 by vol.) to yield **4** as a colorless oil (132 mg; 20%).  $^1\text{H}$  NMR ( $\text{CDCl}_3$ ): 7.1 (m, 6H), 7.0 (m, 2H), 3.9 (m, 3H), 3.2 (s, 4H), 2.6 (m, 2H), 2.4 (s, 3H).  $^{13}\text{C}$  NMR ( $\text{CDCl}_3$ ): 148.3, 134.3, 130.1, 126.7, 123.1, 120.1, 66.9, 55.8,

55.4, 36.5, 32.3. MS (TOF) 282.12 (anal.) 282.17 (calcd).  $[\alpha]_{\text{D}} -4.8^\circ$  ( $c$  10, MeOH).

**5.1.1.4. (R)-1-(10,11-Dihydro-dibenz[b,f]azepin-5-yl)-3-amino-propan-2-ol (8).** A mixture of the alcohol **7** (450 mg; 1.0 mmol), Pearlman's catalyst ( $\text{Pd}(\text{OH})_2$  on carbon; 90 mg; 0.1 mmol) and ammonium formate (605 mg; 4.01 mmol) in methanol (5 mL) was refluxed for 3 h. The catalyst was then removed by filtration, the filtrate concentrated and purified by flash chromatography on silica gel ( $\text{CH}_2\text{Cl}_2 \rightarrow \text{CH}_2\text{Cl}_2\text{-MeOH-c. NH}_4\text{OH}$ , 9:1:0.1 by vol.) to yield **8** as a pale oil (190 mg; 71%).  $^1\text{H}$  NMR ( $\text{DMSO-}d_6$ ): 7.1 (m, 6H), 6.9 (m, 2H), 3.8 (m, 2H), 3.6 (m, 1H), 3.1 (s, 4H), 2.9 (dd,  $J = 4.2, 12.5$  Hz, 1H), 2.7 (m, 1H).  $^{13}\text{C}$  NMR ( $\text{DMSO-}d_6$ ): 148.5, 134.1, 130.2, 126.3, 123.1, 120.2, 64.9, 54.8, 43.5, 31.8. MS (TOF) 268.2079 (anal.) 268.1576 (calcd)  $[\alpha]_{\text{D}} -9.8^\circ$  ( $c$  11, MeOH).

**5.1.1.5. (S)-1-(10,11-Dihydro-dibenz[b,f]azepin-5-yl)-3-methylamino-propan-2-ol (9).** This compound was prepared in the same way as its *R*-enantiomer (**4**), except that the reaction sequence began with (*R*)-epichlorohydrin, and gave the same NMR and MS data.  $[\alpha]_{\text{D}} +6.3^\circ$  ( $c$  8, MeOH).

## 5.2. Radiochemistry

$^{11}\text{C}$ Methane was produced at the Karolinska Hospital with a PETtrace cyclotron (GE Medical Sciences) using 16 MeV protons for the  $^{14}\text{N}(p, \alpha)^{11}\text{C}$  reaction on nitrogen gas containing 10% hydrogen.<sup>34</sup>  $^{11}\text{C}$ Methane was isolated from the target gas on a liquid nitrogen-cooled Porapak<sup>®</sup> Q trap and subsequently converted into  $^{11}\text{C}$ methyl iodide by radical iodination in a recirculation system as previously described.<sup>35</sup>  $^{11}\text{C}$ Methyl triflate was prepared by sweeping  $^{11}\text{C}$ methyl iodide vapour through a heated glass column containing silver-triflate-impregnated graphitized carbon.<sup>36</sup>

Preparative HPLC was performed on a  $\mu$ -Bondapak C-18 column (300  $\times$  7.8 mm, 10  $\mu\text{m}$ ; Waters). The column eluate was passed at 6 mL/min through an absorbance detector ( $\lambda = 254$  nm) preceding a GM-tube for radiation detection. (*R*)- $^{11}\text{C}$ OHDMI and  $^{11}\text{C}$ CFMME were purified with mobile phase A (MeCN– $\text{H}_3\text{PO}_4$  (10 mM), 30:70 v/v) and mobile phase B (MeCN– $\text{NH}_4\text{CO}_2\text{H}$  (0.1 M); 40:60 v/v), respectively.

The radiochemical purity of each product was determined by HPLC on a  $\mu$ -Bondapak C-18 column (300  $\times$  3.9 mm, 10  $\mu\text{m}$ ; Waters) equipped with an absorbance detector ( $\lambda = 214$  and 254 nm for (*R*)-OHDMI and CFMME, respectively) in series with a  $\beta$ -flow detector (Beckman) for radiation detection. (*R*)- $^{11}\text{C}$ OHDMI and  $^{11}\text{C}$ CFMME were analyzed using mobile phase C (MeCN– $\text{H}_3\text{PO}_4$  (10 mM), 30:70 v/v) and mobile phase D (MeCN– $\text{H}_3\text{PO}_4$  (10 mM), 35:65 v/v) at 3 mL/min, respectively.

Radiochemical yields were determined by HPLC analysis of reaction mixtures using the same conditions as described for radiochemical purity determinations.

**5.2.1. [*N*-Methyl-<sup>11</sup>C](*R*)-1-(10,11-dihydro-dibenz[*b,f*]azepin-5-yl)-3-methylamino-propan-2-ol ([<sup>11</sup>C](*R*)-OHDMI; [<sup>11</sup>C]4).** [<sup>11</sup>C]Methyl triflate was trapped at room temperature in a reaction vessel containing the amine precursor **8** (0.3 mg; 1.1 μmol) in acetone (300 μL) (Scheme 2). After entrapment was complete, mobile phase A (600 μL) was added to the reaction mixture before its injection onto preparative HPLC. The fraction eluting at 6 min was collected and mobile phase evaporated off. The residue was taken up in sterile disodium phosphate-buffered saline (pH 7.4; 8 mL) and filtered through a sterile Millipore filter (0.22 μm), yielding [<sup>11</sup>C]4 in sterile solution.

**5.2.2. [*O*-Methyl-<sup>11</sup>C](*S,S*)-1-cyclopentyl-2-(5-fluoro-2-methoxy-phenyl)-1-morpholin-2-yl-ethanol ([<sup>11</sup>C]CFMME; [<sup>11</sup>C]5).** [<sup>11</sup>C]Methyl iodide was trapped at 90 °C in a reaction vessel containing the phenolic precursor **9** (1.0 mg; 3 μmol) and aqueous sodium hydroxide (6 μL; 5 M) in *N,N*-dimethylformamide (400 μL) (Scheme 3). After entrapment was complete, mobile phase B (600 μL) was added to the crude reaction mixture before its injection onto preparative HPLC. The fraction eluting at 7 min was collected and mobile phase evaporated off. The residue was taken up in sterile disodium phosphate-buffered saline (pH 7.4; 8 mL) and filtered through a sterile millipore filter (0.22 μm), yielding [<sup>11</sup>C]5 in sterile solution.

### 5.3. *clog P* calculations and *log D*<sub>7.4</sub> measurements

*clog P* and *clog D*<sub>7.4</sub> values were calculated with the Pallas 3.0 for Windows software (CompuDrug International Inc., San Francisco, CA, USA). *log D*<sub>7.4</sub> was also empirically determined according to the method described by Wilson et al.<sup>37</sup>

### 5.4. Pharmacology

The selectivity and affinities of the ligands in this paper were determined by two assays. The selectivity was determined from an assay on cloned human transporter proteins provided by the National Institute of Mental Health's Psychoactive Drug Screening Program (NIMH PDSP). The affinities of CFMME, (*R*)-OHDMI and (*S,S*)-MeNER for NET were determined by NovaScreen Biosciences Inc. (Hanover, MD, USA). Inhibition constants were obtained from binding curves derived from duplicate measurements at eight different concentrations of inhibitor in the range  $5.0 \times 10^{-10}$  to  $1.0 \times 10^{-6}$  M on rat forebrain membranes.<sup>38</sup>

### 5.5. PET measurements

A Siemens ECAT EXACT HR PET camera (FWHM: about 3.3 mm)<sup>39</sup> was run in 3D mode. Images were displayed as 47 horizontal sections of brain with a separation of 3.3 mm.

Two cynomolgus monkeys (3395 and 3450 g) were supplied by the National Institute for Infectious Disease Control (Solna, Sweden). The study was approved by the Animal Ethics Committee of Northern Stockholm.

Anaesthesia was induced and maintained by repeated intramuscular injection of a mixture of ketamine (3–4 mg kg<sup>-1</sup> h<sup>-1</sup> Ketalar®, Parke-Davis) and xylazine hydrochloride (1–2 mg kg<sup>-1</sup> h<sup>-1</sup> Rompun® vet., Bayer, Sweden). A fixation system was used to secure a position of the monkey head during the PET measurements.<sup>40</sup> Rectal temperature was continuously monitored by an electric thermometer during the PET examinations (Precision thermometer 4600, Harvard Applications, MA, US), and was maintained between 36 and 37 °C by a heating blanket (Bair Hugger—Model 505, Arizant Healthcare Inc, MN, US). In PET measurements, a monkey was injected with [<sup>11</sup>C]CFMME (50 MBq; 1.35 mCi) or (*R*)-[<sup>11</sup>C]OHDMI (52 MBq; 1.41 mCi) as a bolus injection into the left sural vein. Radioactivity in brain was measured according to a pre-programmed sequence of frames during 93 min.

Regions of interest (ROIs) (lower brainstem, mesencephalon, striatum, thalamus, temporal cortex, a region containing locus coeruleus and whole brain) were drawn on summation images reconstructed for a sum of all frames and were defined according to an atlas of a cryosected Cynomolgus monkey head *in situ*.<sup>40</sup> Radioactivity was standardized to a 50 MBq (1.35 mCi) injected dose, calculated for the sequence of time frames, corrected for radioactive decay and plotted versus time. The percentage of injected radioactivity present in brain at the time of maximal radioactivity concentration was used as an index of radioligand uptake into the brain. This percentage was calculated by multiplying the brain volume (about 70 mL) with the radioactivity concentration in the ROI for the whole brain divided by the injected radioactivity. The brain volume was calculated by multiplying the sum of the whole brain regions of all PET-sections with the plane separation.

Striatum, which is a region almost devoid of NET,<sup>1,41,42</sup> was used as a reference region for the free radioligand concentration and non-specific binding in brain for analysis of PET data from (*R*)-[<sup>11</sup>C]OHDMI. To calculate specific binding, radioactivity in the striatum was subtracted from the radioactivity in a ROI. For analysis of PET data from the use of [<sup>11</sup>C]CFMME, striatum could not be used as a reference region since it contained a higher level of radioactivity than some other ROIs (e.g., cerebellum) over the time course of the PET experiment. Hence, cerebellum was used as a surrogate reference ROI.

### 5.6. Analysis of radioactive metabolites in plasma and determination of free fraction

The HPLC method used here to determine the percentages of radioactivity in monkey plasma corresponding to unchanged radioligand and to radioactive metabolites was adapted from a method applied to other PET radioligands.<sup>43</sup>

The HPLC system consisted of an interface module (D-7000; Hitachi), a L-7100 pump (Hitachi), an injector (model 7125 with a 1.0 mL loop; Rheodyne) equipped with a μ-Bondapak-C18 column (300 × 7.8 mm, 10 μm; Waters) and an absorbance detector (L-7400; 254 nm;

Hitachi) in series with a radiodetector (Radiomatic 150TR; Packard) equipped with a PET Flow Cell (600  $\mu$ L). Phosphoric acid (10 mM) (E) and acetonitrile (F) were used as mobile phase components. The program for gradient elution (6 mL/min) was; 0–5.5 min, (E/F) 90/10  $\rightarrow$  40/60; 5.5–6.5 min, (E/F) 40/60  $\rightarrow$  90/10; 6.5–10 min (E/F) 90/10.

Venous blood samples (2 mL) were obtained from the monkey subject at 4, 15 and 30 min after radioligand injection and centrifuged at 2000g for 2 min Supernatant plasma (0.5 mL) was mixed with acetonitrile (0.7 mL) and injected onto the HPLC-system. The radioactive peak having a retention time corresponding to reference ligand was integrated and its area expressed as a percentage of the sum of the areas of all detected radioactive peaks (decay-corrected).

The free fraction of [ $^{11}$ C]CFMME and (R)-[ $^{11}$ C]OHD-MI was determined by ultrafiltration.<sup>44</sup> The appropriate radioligand ( $\sim$ 20  $\mu$ L) was incubated with monkey plasma (500  $\mu$ L) for 10 min at RT, after which the incubate was pipetted into ultrafiltration units (Centrifree, Waters) and spun for 20 min at 4000 rpm. To correct for radioligand retention in ultrafiltration units, saline solutions were incubated with radioligand and processed identically to that described above. The free fraction was calculated as the decay-corrected ratio between radioactivity in equal volumes (200  $\mu$ L) of spun and unspun plasma (corrected for retention in ultrafiltration units).

### Acknowledgment

The authors thank Mr. Arsalan Amir, Mr. Phong Truong and other members of the PET group at the Karolinska Institutet. This study was supported in part by the Intramural Research Program of the National Institutes of Health (NIH), specifically the National Institute of Mental Health (NIMH), and was also performed under a CRADA agreement between NIMH, the Karolinska Institutet and Eli Lilly and Co. Dr. M. Schou also received support through the National Institutes of Health-Karolinska Institutet graduate training partnership in neuroscience. The authors are also grateful to the NIMH PDSP for performing assays. The NIMH PDSP is directed by Bryan L. Roth, PhD, and project officer Jamie Driscoll at NIMH at the University of North Carolina at Chapel Hill; Contract # NO1MH32004.

### References and notes

- Donnan, G.; Kaczmarczyk, S.; Paxinos, G.; Chilco, P.; Kalnins, R.; Woodhouse, D.; Mendelsohn, F. *J. Comp. Neurol.* **1991**, *304*, 419–434.
- Ordway, G.; Stockmeier, C.; Cason, G.; Klimek, V. *J. Neurosci.* **1997**, *17*, 1710–1719.
- Tejani-Butt, S.; Yang, J.; Zaffar, H. *Brain Res.* **1993**, *631*, 147–150.
- Ressler, K.; Nemeroff, C. B. *Biol. Psychiatry* **1999**, *46*, 1219–1233.
- Klimek, V.; Stockmeier, C.; Overholser, J.; Meltzer, H.; Kalka, S.; Dilley, G.; Ordway, G. *J. Neurosci.* **1997**, *17*, 8451–8458.
- Brunello, N.; Mendlewicz, J.; Kasper, S.; Leonard, B.; Montgomery, S.; Nelson, J.; Paykel, E.; Versiani, M.; Racagni, G. *Eur. Neuropsychopharmacol.* **2002**, *12*, 461–475.
- Spencer, T.; Heiligenstein, J.; Biederman, J.; Faries, D.; Kratochvil, C.; Conners, C.; Potter, W. *J. Clin. Psychiatry* **2002**, *63*, 1140–1147.
- Haka, M.; Kilbourn, M. *Nucl. Med. Biol.* **1989**, *16*, 771–774.
- Schou, M.; Sovago, J.; Pike, V. W.; Gulyas, B.; Bogeso, K. P.; Farde, L.; Halldin, C. *Mol. Imaging Biol.* **2005**, 1–8.
- Kiyono, Y.; Kanegawa, N.; Kawashima, H.; Kitamura, Y.; Iida, Y.; Saji, H. *Nucl. Med. Biol.* **2004**, *31*, 147–153.
- Kung, M. P.; Choi, S. R.; Hou, C.; Zhuang, Z. P.; Foulon, C.; Kung, H. F. *Nucl. Med. Biol.* **2004**, *31*, 533–541.
- Ding, Y. S.; Lin, K. S.; Logan, J.; Benveniste, H.; Carter, P. *J. Neurochem.* **2005**, *94*, 337–351.
- McConathy, J.; Owens, M. J.; Kilts, C. D.; Malveaux, E. J.; Camp, V. M.; Votaw, J. R.; Nemeroff, C. B.; Goodman, M. M. *Nucl. Med. Biol.* **2004**, *31*, 705–718.
- Lin, K.-S.; Ding, Y.-S.; Betzel, T.; Quandt, G. *J. Label Compd. Radiopharm.* **2005**, *48*, S152.
- Schou, M.; Halldin, C.; S ovag o, J.; Pike, V.; Gulyas, B.; Mozley, P.; Johnson, D.; Hall, H.; Innis, R.; Farde, L. *Nucl. Med. Biol.* **2003**, *30*, 707–714.
- Wilson, A.; Johnson, D.; Mozley, P.; Hussey, D.; Ginovart, N.; Nobrega, J.; Garcia, A.; Meyer, J.; Houle, S. *Nucl. Med. Biol.* **2003**, *30*, 85–92.
- Ding, Y. S.; Lin, K. S.; Garza, V.; Carter, P.; Alexoff, D.; Logan, J.; Shea, C.; Xu, Y.; King, P. *Synapse* **2003**, *50*, 345–352.
- Schou, M.; Halldin, C.; Sovago, J.; Pike, V. W.; Hall, H.; Gulyas, B.; Mozley, P. D.; Dobson, D.; Shchukin, E.; Innis, R. B.; Farde, L. *Synapse* **2004**, *53*, 57–67.
- Schou, M.; Halldin, C.; Pike, V. W.; Mozley, P. D.; Dobson, D.; Innis, R. B.; Farde, L.; Hall, H. *Eur. Neuropsychopharmacol.* **2005**, *15*, 517–520.
- Hyttel, J. *Prog. Neuro-Psychopharmacol. & Biol. Psychiat.* **1982**, *6*, 277–295.
- Waldmeier, P. C.; Baumann, P. A.; Hauser, K.; Maitre, L.; Storni, A. *Biochem. Pharmacol.* **1982**, *31*, 2169–2176.
- Javaid, J. I.; Perel, J. M.; Davis, J. M. *Life Sci.* **1979**, *24*, 21–28.
- Levy, O.; Erez, M.; Varon, D.; Keinan, E. *Bioorg. Med. Chem. Lett.* **2001**, *11*, 2921–2926.
- Schindler, W.; Hafziger, F. *Helv. Chim. Acta* **1954**, *59*, 472.
- Melloni, P.; Carniel, G.; Della Torre, A.; Bonsignori, A.; Buonamici, M.; Pozzi, O.; Ricciardi, S.; Rossi, A. *Eur. J. Med. Chem. Chim. Ther.* **1984**, *19*, 235–242.
-  ohman, D.; Norlander, B.; Peterson, C.; Bengtsson, F. *Ther. Drug Monit.* **2001**, *23*, 27–34.
- Bergeron, R. J.; Xia, M. X. B.; Phanstiel, O. *J. Org. Chem.* **1993**, *58*, 6804–6806.
- Kobayashi, M.; Hamaguchi, S.; Katayama, K.; Ohashi, T.; Watanabe, K. *Production of carnitine intermediate*. In JP62212352; 1986.
- Dischino, D.; Welch, M.; Kilbourn, M.; Raichle, M. *J. Nucl. Med.* **1983**, *24*, 1030–1083.
- Balle, T.; Halldin, C.; Andersen, L.; Hjorth Alifrangis, L.; Badolo, L.; Gjervig Jensen, K.; Chou, Y. W.; Andersen, K.; Perregaard, J.; Farde, L. *Nucl. Med. Biol.* **2004**, *31*, 327–336.
- Waterhouse, R. N. *Mol. Imaging Biol.* **2003**, *5*, 376–389.
- Smith, H. R.; Beveridge, T. J.; Porrino, L. *J. Neuroscience* **2006**, *138*, 703–714.

33. Cases-Thomas, M. J.; Masters, J. J.; Walter, M. W.; Campbell, G.; Haughton, L.; Gallagher, P. T.; Dobson, D. R.; Mancuso, V.; Bonnier, B.; Giard, T.; Defrance, T.; Vanmarsenille, M.; Ledgard, A.; White, C.; Ouwerkerk-Mahadevan, S.; Brunelle, F. J.; Dezutter, N. A.; Herbots, C. A.; Lienard, J. Y.; Findlay, J.; Hayhurst, L.; Boot, J.; Thompson, L. K.; Hemrick-Luecke, S. *Bioorg. Med. Chem. Lett.* **2006**, *16*, 2022–2025.
34. Bjork, H. In *10th Workshop on Targetry and Target Chemistry*; Madison, Wisconsin, 2004.
35. Någren, K.; Truong, P.; Helin, S.; Amir, A.; Halldin, C. *J. Label Compd. Radiopharm.* **2003**, *46*, S76.
36. Sandell, J.; Langer, O.; Larsen, P.; Dolle, F.; Vaufrey, F.; Demphel, S.; Crouzel, C.; Halldin, C. *J. Label Compd. Radiopharm.* **2000**, *43*, 331–338.
37. Wilson, A. A.; Jin, L.; Garcia, A.; DaSilva, J. N.; Houle, S. *Appl. Radiat. Isot.* **2001**, *54*, 203–208.
38. Raisman, R.; Sette, M.; Pimoule, C.; Briley, M.; Langer, S. Z. *Eur. J. Pharmacol.* **1982**, *78*, 345–351.
39. Wienhard, K.; Dahlbom, M.; Eriksson, L.; Michel, C.; Bruckbauer, T.; Pietrzyk, U.; Heiss, W. *J. Comput. Assist. Tomogr.* **1994**, *18*, 110–118.
40. Karlsson, P.; Farde, L.; Halldin, C.; Swahn, C.-G.; Sedvall, G.; Foged, C.; Hansen, K.; Skrumsager, B. *Psychopharmacology* **1993**, *113*, 149–156.
41. Raisman, R.; Sette, M.; Pimoule, C.; Briley, M.; Langer, S. Z. *Eur. J. Pharmacol.* **1982**, *78*, 345–351.
42. Tejani-Butt, S. *J. Pharm. Exp. Ther.* **1992**, *260*, 427–436.
43. Charnay, Y.; Leger, L.; Vallet, P.; Hof, P.; Juovet, M.; Bouras, C. *Neuroscience* **1995**, *69*, 259–270.
44. Halldin, C.; Swahn, C.-G.; Farde, L.; Sedvall, G. In *Radioligand Disposition and Metabolism*; Comar, D., Ed.; PET for Drug Development and Evaluation; Kluwer Academic Publishers, 1995; pp 55–65.